HHS Public Access

Author manuscript

Circ Heart Fail. Author manuscript; available in PMC 2024 December 19.

Published in final edited form as:

Circ Heart Fail. 2023 December ; 16(12): e010351. doi:10.1161/CIRCHEARTFAILURE.122.010351.

Nonsense Variant PRDM16-Q187X Causes Impaired Myocardial Development and TGF-Beta Signaling Resulting in Noncompaction Cardiomyopathy in Humans and Mice

Bo Sun, PhD[1,a], **Omid M.T. Rouzbehani, MSC**[2,a], **Ryan J. Kramer, BA**[1], **Rajeshwary Ghosh, PhD**[2], **Robin M. Perelli, MS**[3], **Sage Atkins, BS**[1], **Amir Nima Fatahian, BS**[2], **Kathryn Davis, PhD**[4], **Marta W. Szulik, PhD**[4], **Michael A. Goodman, BS**[2], **Marissa A. Hathaway, BS**[2], **Ellenor Chi, BA**[2], **Tarah A. Word, PhD**[5], **Hari Tunuguntla, MD, MPH**[6], **Susan W. Denfield, MD**[6], **Xander H. T. Wehrens, MD, PhD**[5,6,7], **Kevin J. Whitehead, MD**[8], **Hala Y. Abdelnasser, BS**[9], **Junco S. Warren, PhD**[4,10], **Mingfu Wu, PhD**[9], **Sarah Franklin, PhD**[4], **Sihem Boudina, PhD**[2,*], **Andrew P. Landstrom, MD, PhD**[1,3,*]

[1]Department of Pediatrics, Division of Cardiology, Duke University School of Medicine, Durham, North Carolina, United States

[2]Department of Nutrition and Integrative Physiology, Program in Molecular Medicine, University of Utah, Salt Lake City, Utah, United States

[3]Department of Cell Biology, Duke University School of Medicine, Durham, North Carolina, United States

[4]Nora Eccles Harrison Cardiovascular Research and Training Institute, University of Utah, Salt Lake City, Utah

[5]Department of Molecular Physiology & Biophysics, Baylor College of Medicine, Houston, Texas, United States

[6]Departments of Medicine and Pediatrics, Section of Cardiology, Baylor College of Medicine, Houston, Texas, United States

[7]Departments of Neuroscience, Cardiovascular Research Institute, and Center for Space Medicine, Baylor College of Medicine, Houston, Texas, United States

[8]Division Cardiovascular Medicine, Department of Internal Medicine, University of Utah School of Medicine, Salt Lake City, Utah, United States

[*]Co-Corresponding authors: Sihem Boudina, PhD, University of Utah Molecular Medicine Program, 15 N 2030 E Bldg. # 533 Rm. 3410B, Salt Lake City, Utah 84112, Phone: (801) 585-6833, Fax: (801) 585-0701, sboudina@u2m2.utah.edu, Andrew Landstrom, MD, PhD, Duke University School of Medicine, Box #2652, Durham, NC 27278, Phone: (919) 684-3028, Fax: (919) 385-9329, andrew.landstrom@duke.edu.

[a]The authors equally contributed

Disclosures

The authors declare no conflicts of interest or disclosures.

Supplemental Materials:

Supplemental Methods

Tables S1–S5

Figures S1–S6

References 31–57

[9]Department of Pharmacological and Pharmaceutical Sciences, The University of Houston College of Pharmacy, Houston, Texas, United States

[10]Division of Cardiovascular Medicine, University of Utah School of Medicine, Salt Lake City, Utah, United States

Abstract

Background: PRDM16 plays a role in myocardial development through TGFβ signaling. Recent evidence suggests that loss of PRDM16 expression is associated with cardiomyopathy development in mice, although its role in human cardiomyopathy development is unclear. This study aims to determine the impact of PRDM16 loss-of-function variants on cardiomyopathy in humans.

Methods: Individuals with *PRDM16* variants were identified and consented. Induced pluripotent stem cell-derived cardiomyocytes (iPSC-CMs) were generated from a proband hosting a Q187X nonsense variant as an *in vitro* model and underwent proliferative and transcriptional analyses. CRISPR-mediated knock-in mouse model hosting the $Prdm16^{Q187X}$ allele was generated and subjected to echocardiograph, histologic, and transcriptional analysis.

Results: We report two probands with loss-of-function *PRDM16* variants and pediatric left ventricular noncompaction cardiomyopathy (LVNC). One proband hosts a PRDM16-Q187X variant with LVNC and demonstrated infant-onset heart failure which was selected for further study. Induced pluripotent stem cells derived cardiomyocytes (IPSC-CMs) prepared from the PRDM16-Q187X proband demonstrated a statistically significant impairment in myocyte proliferation and increased apoptosis associated with transcriptional dysregulation of genes implicated in cardiac maturation, including TGFβ-associated transcripts. Homozygous $Prdm16^{Q187X/Q187X}$ mice demonstrated an underdeveloped compact myocardium and were embryonic lethal. Heterozygous $Prdm16^{Q187X/WT}$ mice demonstrated significantly smaller ventricular dimensions, heightened fibrosis, and age-dependent loss of TGFβ-expression. Mechanistic studies were undertaken in H9c2 cardiomyoblasts to show that PRDM16 binds TGFB3 promoter and represses its transcription.

Conclusion: Novel loss-of-function *PRDM16* variant impairs myocardial development resulting in noncompaction cardiomyopathy in humans and mice associated with altered TGFβ signaling.

Visual Overview: An online visual overview is available for this article.

Keywords

cardiomyopathy; cardiac maturation; transcription; genetic variants; induced pluripotent stem cells; TGFβ signaling

INTRODUCTION

Left ventricular non-compaction (LVNC) is a primary disease of the heart muscle characterized by the presence of dense trabeculations within the left ventricle, which appear “non-compacted” on echocardiography[1]. LVNC is associated with a high incidence of morbidity and mortality, with 47% of adult patients (and 75% of symptomatic patients)

dying within 6 years of diagnosis, often due to ventricular arrhythmias leading to sudden death[2]. While LVNC is believed to have a genetic basis, only 15–25% of patients have identifiable genetic mutations[3]. This lack of known genetic and molecular mechanisms has impeded the progress of medical therapies for the management and prevention of LVNC-related mortality.

Pediatric cardiomyopathy is a rare but highly morbid and potentially lethal childhood cardiovascular disease. Cardiomyopathy affects at least 1 in 100,000 children in the United States with the greatest incidence in those less than 1 year old[4]. Among those with symptomatic cardiomyopathy, 40% undergo heart transplantation or die from cardiac complications within 2 years[4]. Cardiomyopathy is phenotypically heterogeneous with a broad scope of potential causes. Despite this, the majority of individuals with cardiomyopathic disease are due to potentially heritable genetic variants in a large number of genes. Several genes, mostly encoded elements of the cardiac sarcomere, have been implicated in the development of cardiomyopathy; yet, many genetic causes are still undetermined[5]. One recent retrospective study found clinical genetic testing identified pathological variants in only 26% of cases[6]. Consequently, further work has targeted identification of cardiomyopathic loci and prediction of pathogenicity in variants of undetermined significance in order to better understand the genetic landscape of pediatric cardiomyopathy[7].

1p36 deletion syndrome is the most common terminal chromosomal deletion associated with neurological impairments, craniofacial anomalies, and cardiovascular defects notable for cardiomyopathy[8, 9]. Thus, 1p36 deletion syndrome is a fruitful research target for cardiomyopathy genetics research as it contains a known cardiomyopathic locus within a limited set of genes to index. One such locus is *PRDM16*, a transcription factor linked to inherited cardiomyopathy in 1p36 deletion syndrome[10]. This remains controversial as there are other potential cardiomyopathic loci in the 1p36 region that confound the effects of PRDM16 loss[11]. In order to better understand effects of isolated *PRDM16* loss, several cardiac conditional knockout mouse models have been generated, all of which demonstrate cardiomyopathy[12–16]. These studies identify a role for PRDM16 in canonical TGFβ signaling wherein loss of *PRDM16* results in an overall increase in this signaling pathway[12–14]. However, these models demonstrate variable clinical phenotypes, including hypertrophy, LV dilation, and LV noncompaction (LVNC)[12–16]. Further, it remains unknown if these murine models translate to humans. Specifically, the mechanism behind cardiomyopathy development in patients with *PRDM16* mutations has yet to be determined.

In this study, we identify two pediatric probands hosting isolated loss-of-function *PRDM16* variants and who developed LVNC and quickly progressed into heart failure. We next generated mice with a human *PRDM16* variant (Proband 1's PRDM16-Q187X variant) and confirmed that Prdm16 loss causes LVNC and pathological remodeling. Using human induced pluripotent stem cell-derived cardiomyocytes (hiPSC-CMs) from Proband 1 and Prdm16-Q187X knock in mouse model, we demonstrate that PRDM16 regulates proliferation of cardiomyocytes in humans and mice. We also reveal a cell-autonomous regulation of TGFβ signaling by PRDM16 in cardiac cells. This work provides the first

investigation of *PRDM16* loss in humans and provides insights into the mechanisms by which *PRDM16* causes LVNC.

METHODS

The authors declare that all supporting data are available within the article and its online supplementary files. All RNA sequencing data is available in NCBI: Gene Expression Omnibus under accession N GSE193878. Raw sequencing data can be made available upon request.

This study received approval from the Institutional Review Boards at Baylor College of Medicine and Duke University Health System and all cases and patient-derived lines were obtained following receipt of informed consent. Animal studies were conducted in strict accordance with the National Institutes of Health guidelines for humane treatment of animals and approved by the Institutional Animal Care and Use Committee at the University of Utah and Duke University, respectively. A detailed methods section is available in the Supplemental Materials.

Statistics

All data are presented as the mean ± SD; $p < 0.05$ were considered significant, unless otherwise noted. Statistical analysis was performed with GraphPad. Unpaired Student's t test was used to compare two independent groups with the exception of the mouse genotypes in which contingency tables were used. One-way ANOVA with Tukey post hoc test was used for multiple group analysis. Mendelian ratios were compared using Chi-square testing. Investigators were blinded to genotype during data collection and analysis.

RESULTS

Loss-of-function pathogenic variants in *PRDM16* are associated with LVNC and pediatric heart failure in humans

While the loss of the *PRDM16* genetic locus has been suggested as the needed trigger for the development of LVNC associated with 1p36 deletion syndrome in humans[10], the concomitant deletion of other genes proximal to the *PRDM16* locus has left it unclear whether it is both necessary and sufficient to cause LVNC. Using whole exome sequencing, we identified two putative loss-of-function variants in two unrelated pediatric patients with LVNC with likely pathogenic variants in *PRDM16*. Proband 1 is a male child who demonstrated LV trabeculations on echocardiography at 4 days of life without a family history of cardiac disease (Fig 1a). Repeat echocardiography at 3 months of age demonstrated prominent trabeculations, consistent with LVNC, and development of marked LV dilation and severe loss of systolic function (Fig 1b and Table S1). Traditional gene panel testing for all known cardiomyopathy-associated genes did not identify a disease-associated variant. Exome sequencing identified a heterozygous nonsense variant in exon 4 of the *PRDM16* gene (PRDM16-Q187X, *PRDM16-c.559C>T,* NM_022114, Fig 1c). This variant was predicted to cause an early termination of translation within the N-terminal PR domain of PRDM16 (Fig S1a). Exome sequencing excluded the presence of a rare variant in any other genetic loci within the 1p36 region potentially associated with cardiomyopathy (i.e.

SKI, GABRD, and *MMP23B*). The variant was absent in over 280,000 control/reference alleles placing the minor allele frequency at <4E-6 in the general population (gnomAD), absent in ClinVar, and not previously reported. The PRDM16-Q187X variant is predicted to be deleterious by a series of *in silico* pathogenicity models (Table S2) and was deemed likely pathogenic by ACMG criteria. The proband had no extra-cardiac features, including those associated with 1p36 deletion syndrome. Cascade genetic evaluation of this variant found it to be absent in biological parents, indicating a *de novo* mode of inheritance. Overexpression of this variant in HEK293T cells confirmed a loss of full-length protein expression (Fig 1d). This variant represents the first nonsense variant described in *PRDM16* linked to pediatric LVNC and pediatric onset heart failure.

A second loss-of-function variant was identified in a 5-year-old female child (Proband 2) who was diagnosed with LVNC and had no family history of cardiovascular disease (Fig 1e). Echocardiogram demonstrated prominent trabeculations, consistent with LVNC, and otherwise normal LV dimensions and preserved cardiac systolic function (Fig 1f). Diagnostic cardiomyopathy gene panel testing was negative; however, exome sequencing identified a heterozygous splice variant in the 3' junction of exon 5 of the *PRDM16* gene (*PRDM16-c.676+2T>C,* NM_022114, Fig S1b). As with Proband 1, exome sequencing confirmed the absence of rare variants in other genes within the 1p36del locus. Moreover, the variant was absent in gnomAD and ClinVar, deemed likely pathogenic by ACMG criteria, and never reported or described. Cascade genetic testing confirmed a *de novo* mode of inheritance. Overall, this identification of a second, unrelated proband with a presumptive loss-of-function variant in *PRDM16* supports the conclusion that these variants are a rare cause of pediatric-onset LVNC and heart failure. To determine the mechanism of loss-of-function variants in *PRDM16*, we selected the nonsense mutation to further define underlying mechanisms of disease development given its location within the coding sequence of the gene locus.

PRDM16-Q187X is associated with reduced proliferation and increased apoptosis in iPSC-derived cardiomyocytes

To identify the developmental defects associated with loss-of-function variants, we first generated induced pluripotent stem cell (iPSC) lines derived from the proband carrying the PRDM16-Q187X variant ($iPSC^{QX/WT}$). These iPSCs had a normal karyotype, carried the Q187X variant by Sanger sequencing, and expressed the anticipated pluripotency markers (Fig S2a–c). As a control, we used both a non-isogenic healthy control individual ($iPSC^{WT/WT}$) as well as a CRISPR-corrected line ($iPSC^{cWT/WT}$) (Table S3). Differentiation into iPSC-derived cardiac myocytes (iPSC-CMs) was validated by cell morphology, spontaneous beating in coordinate syncytia, and robust expression of TNNT2, ACTC1 (Fig 2a), downregulation of pluripotency markers and increased expression of cardiac-specific markers by immunofluorescence and qPCR (Fig S2d–f). $IPSC\text{-}CMs^{QX/WT}$ demonstrated PRDM16 expression predominantly in the nucleus with weaker expression in the cytosol which was similar to both control lines (Fig 2b). Quantification of *PRDM16* expression in the $iPSC\text{-}CMs^{QX/WT}$ found reduced expression compared to controls without a corresponding decrease in *PRDM16* transcript by qPCR (Fig 2c–d, Table S4). These

findings suggest that PRDM16-Q187X results in decreased PRDM16 expression by nonsense mediated decay.

We next explored whether there was evidence of cardiomyopathic cellular remodeling. We found robust and equivocal expression of ACTC1 in iPSC-CMs$^{QX/WT}$ compared to control lines (Fig 2e). Conversely, while control iPSC-CMs$^{WT/WT}$ and iPSC-CMs$^{cWT/WT}$ demonstrated organized, parallel arrays of sarcomeric TNNT2, iPSC-CMs$^{QX/WT}$ demonstrated an abnormal organization of TNNT2 with loss of parallel myofilament alignment. In addition, the percentage of cells that were positive for TNNT2 expression was lower in iPSC-CMs$^{QX/WT}$ compared to controls (Fig 2f–g) with a corresponding decrease in *TNNT2* expression by qPCR (Fig 2h). To assess the cell proliferation potential in maturing iPSC-CMs, the distribution of S-phase cardiomyocytes was determined by EdU incorporation. IPSC-CMs$^{QX/WT}$ demonstrated reduced proliferation capacity by ~ 30% relative to both control lines (Fig 2i–j). Further, TUNEL staining was performed to analyze apoptosis and demonstrated an increase in apoptosis in iPSC-CMs$^{QX/WT}$ compared with control cells (Fig 2k–l). Given this, we next evaluated markers of cardiomyopathic remodeling[12, 14] and found that *NPPA* and *NPPB* had significantly higher expression of these markers compared with control lines (Fig 2m–n). Taken together, these results suggest that the PRDM16-Q187X variant is associated with impaired myocyte proliferation and increased apoptosis associated with cellular cardiomyopathic remodeling.

Prdm16$^{QX/QX}$ knock-in mice develop ventricular noncompaction, decreased cardiomyocyte proliferation with reduced cell size, and die before birth

To validate whether loss-of-function mutations in *PRDM16* were sufficient to cause cardiomyopathy in a corresponding *in vivo* model, we generated the Gln187Ter variant allele in *Prdm16* in a C57BL/6NJ background using CRISPR-Cas9-mediated genome editing (Fig 3a–c). With *Prdm16*$^{QX/WT}$ × *Prdm16*$^{QX/WT}$ in-crossing, there were no homozygous mutant mice (*Prdm16*$^{QX/QX}$) born alive and were presumed embryonic lethal (Fig S3a). With *Prdm16*$^{QX/WT}$ × *Prdm16*$^{WT/WT}$ in-crossing, the numbers of pups born are not different from the numbers expected from the Mendelian law, overall (Fig S3b, Table S5). Interestingly, there was a slightly lower than anticipated proportion of female *Prdm16*$^{QX/WT}$ mice born, with only 40% of *Prdm16*$^{QX/WT}$ mice being female compared to 49% of control *Prdm16*$^{WT/WT}$ mice (Fig S3c, Table S5). Following birth, *Prdm16*$^{QX/WT}$ heterozygous mice had normal survival without noticeable functional impairment compared to *Prdm16*$^{WT/WT}$ controls. Expression analysis of Prdm16 at P3 and 3 months among *Prdm16*$^{QX/WT}$ mice demonstrated similar mRNA expression compared to controls (Fig S3d). Given the embryonic lethality noted, we next performed histologic analysis of embryonic (E16.5) *Prdm16*$^{QX/QX}$ hearts. While we found no structural defects of the heart, and trabecular layer of the myocardium appeared normally developed, the compacted layer was thinner in *Prdm16*$^{QX/QX}$ embryos compared with both *Prdm16*$^{QX/WT}$ and *Prdm16*$^{WT/WT}$ embryos (Fig 3d). This thinner compacted myocardium was associated with reduced Ki67^{+} positive cells and had the overall impact of increasing the relative thickness of the trabecular myocardium to compacted myocardium, a hallmark of LVNC in humans (Fig 3e–i). To further confirm this finding, we next stained fetal heart sections for phospho-histone H3 (PH3)-positive cardiomyocytes in the compact and trabecular

layers finding a lower number of PH3-positive myocytes in both among *Prdm16*$^{QX/QX}$ hearts. Moreover, when stained with wheat germ agglutinin (WGA), *Prdm16*$^{QX/QX}$ hearts demonstrated reduced cardiac myocyte size, measured in cross-sectional area, compared with both *Prdm16*$^{QX/WT}$ and *Prdm16*$^{WT/WT}$ embryos (Fig 4a–e). These results suggest that PRDM16-Q187X causes developmental arrest of cardiomyocytes as well as smaller cardiac myocytes which results in under development of the compacted myocardium and an embryonic lethal noncompaction cardiomyopathy.

Given these findings in the developing heart, we next evaluated the *Prdm16*$^{QX/WT}$ mice for evidence of cardiomyopathy through blinded echocardiography analysis at 3 and 8 months of age. *Prdm16*$^{QX/WT}$ mice demonstrated smaller LV internal dimensions, particularly during systole with increased fractional shortening, and decreased predicted stroke volumes (Fig 5a–e) throughout each of the ages analyzed. These measurements resulted in a reduced calculated left ventricular (LV) mass in *Prdm16*$^{QX/WT}$ mice (Fig S4a–d). Histological examination using Masson's Trichrome and Hematoxylin and Eosin staining at 3 and 8 months revealed that *Prdm16*$^{QX/WT}$ mice have a smaller ventricular chamber volume with trabecular/noncompacted myocardium as well as significantly increased fibrosis compared to controls (Fig 5f–j, Fig S4e–f). These histological changes were associated with elevation of *Nppa* and *Nppb* mRNA expression at 3 months which was not present at P3, suggesting the development of cardiac remodeling late in adulthood (Fig 5k–l). Overall, these results suggest that loss of PRDM16 results in impaired myocardial development of the ventricles with resultant noncompaction cardiomyopathy with myocardial fibrotic remodeling that develops in the adult mouse.

PRDM16-Q187X is associated with modulation of developmentally-dependent *TGFβ* signaling

We hypothesized that loss of *PRDM16* will lead to overexpression of TGFB, given the previously identified role of PRDM16 in negative regulation of canonical TGFβ signaling which is needed for myocardial development[17, 18]. Moreover, activation of TGFβ signaling was also seen in human iPSC-CMs derived from patients with LVNC carrying variant in the transcription factor TBX20[19]. Recently, perturbations in regulation of TGFβ signaling in Prdm16-deficient hearts were demonstrated by us and others[12–15]. However, none of these studies examined the mechanisms by which loss-of-function PRDM16 mutations regulate TGFB genes. To determine this, we first conducted gene expression analysis by RNA sequencing (RNA-seq) of iPSC-CM$^{QX/WT}$ and iPSC-CM$^{WT/WT}$ which yielded 298 differentially expressed genes with 170 upregulated and 128 downregulated genes (Fig 6a). To take advantage of our complementary mouse model, RNA-seq analysis of left ventricular myocardium from Prdm16$^{QX/WT}$ mice at P3 and 3 months were compared to controls and identified altered expression of 89 genes with 73 upregulated and 16 downregulated genes at P3 (Fig 6b), and 70 genes with 37 upregulated and 33 downregulated genes at 3 months (Fig 6c). We next combined this analysis to identify pathways common to both iPSC-CMs and *Prdm16* mice. Kyoto Encyclopedia of Genes and Genomes (KEGG) analysis revealed common downregulated pathways in cardiac muscle contraction with genes encoding contractile proteins being over-represented (*MYL2*, *MYL3*, *MYH7* and *TNNI3*), oxidative phosphorylation (*COX7A1*, *SDHA*, *NDUFS6* and *NDUFS2*) and TCA

cycle (*IDH3A*, *CS*, *ACO2*, *DLD*, *IDH2*, *DLAT* and *PDHA1*). We also detected alterations in cardiac developmental regulators including downregulated NOTCH genes (*DLL3*, *DLL4*, *NUMB* and *JAG1*) in the iPSC-CMs from the proband and an upregulation of hedgehog genes (*Bmp2*, *Wnt2*, *Gli1*, *Sufu* and *Smo*) in *Prdm16*$^{QX/WT}$ hearts (Fig 6d).

In addition to these global developmental pathways, transcriptome analysis found TGFβ signaling to be markedly down-regulated in P3 Prdm16$^{QX/WT}$ mice compared to controls. Interestingly, this reduced TGFβ expression shifts in the 3-month-old adult Prdm16$^{QX/WT}$ mice to increased expression relative to controls. This increase in TGFβ expression was also noted in the iPSC-CM$^{QX/WT}$ compared to controls (Fig 6d). This developmentally dynamic change in expression was supported by confirmatory qPCR which found an overall decrease in mRNA expression of several TGFβ signaling molecules in P3 Prdm16$^{QX/WT}$ mice vs controls, including *Tgfb2, Tgfbr1, Tgfbr2*, which then increased at 3 months (Fig 6e–h). Furthermore, iPSC-CM$^{QX/WT}$ showed significant upregulation of TGFβ signaling-related genes compared with both iPSC-CM$^{WT/WT}$ and CRISPR-corrected isogenic iPSC-CMs$^{cWT/WT}$ (Fig 6i–j). Taken together, these results suggest that TGFβ is a critical signaling pathway in PRDM16-mediated disease. Moreover, PRDM16-Q187X suppressed TGFβ signaling early in development, when there is associated impaired myocardial development, which then increased later in the adult heart with associated cardiomyopathic remodeling.

Cell autonomous regulation of *Tgfb2* and *Tgfb3* genes by Prdm16 in cardiac cells

To examine whether Prdm16 directly represses TGFB-associated genes in a cell autonomous fashion, and whether this regulation occurs via modulation of the promoter activity of TGFB genes, we used Prdm16 loss-and-gain-of-function studies in rat cardiac H9c2 cardiomyoblasts. Knockdown of *Prdm16* with siRNA enhanced, whereas its overexpression reduced, both *Tgfb2* and *Tgfb3* mRNA expression, respectively (Fig 7a, c). Similarly, the mRNA expression of *Tgfb2* and *Tgfb3* was elevated in neonatal rat cardiomyocytes (NRVMs) with *Prdm16* knockdown (Fig 7b). PRDM16 regulates transcription through several mechanisms involving either direct binding to the promoter of genes, by indirectly modulating chromatin or *via* interaction with DNA binding proteins[20]. Thus, depending on the specific mode of regulation, PRDM16 can activate or repress gene expression in a tissue and a time-dependent manner. To assess how PRDM16 inhibits *TGFB* gene expression we performed chromatin immunoprecipitation (ChIP)-PCR assays in gain-of-function experiments. Three primer sets were designed in the promoter region of *Tgfb3* and *Tgfb2* based on published H3K4 and H3K9 methylation enrichment patterns from ChIP-sequencing of human heart tissue (WashU EpiGenome database, epigenomegateway.wustl.edu) (Fig 7d, e, Fig S5a, b). Using these primers, we performed ChIP-PCR of Myc-tagged PRDM16 expressed via adenovirus in H9c2 cells and confirmed binding at the *Tgfb3 and Tgfb2* promoter (Fig 7f, Fig S5c) as well as an increase in histone 3 lysine 4 monomethylation (H3K4me1) and a decrease in histone 3 lysine 4 trimethylation (H3K4me3) at this same region (Fig 7g, h, Fig S5d–f). In contrast, siRNA knockdown of PRDM16 in these cells, reduced H3K4me1 and H3K9me3, and enhanced H3K4me3 marks in *Tgfb3* promoter region (Fig S5g–i, Fig S6a–c). ChIP-PCR against random intergenic region or *Tbp* control gene that is not targeted by PRDM16 shows a lack of enrichment

therefore supports specificity in targeting. These results suggest that Prdm16 regulates *Tgfb2* and *Tgfb3* expression *via* its methyltransferase activity by mono-methylating H3K4.

DISCUSSION

PRDM16 is a transcriptional regulator implicated in cellular differentiation and is suspected to play a role in cardiac specification from mouse and zebrafish studies[10],[12–15]. In humans, PRDM16 has been studied in association with 1p36 deletion syndrome, a chromosomal deletion syndrome in which *PRDM16* can be lost and with which cardiomyopathy has been associated[10],[21]. However, the role of PRDM16 in human hearts remains unclear and loss-of-function *PRDM16* variants have not been fully characterized. In this study we sought to determine the effects of *PRDM16* variants in cardiomyocytes and the pathogenesis of cardiomyopathy. To do so, we examined how PRDM16 modulates transcription using human iPSC-CMs and mouse heart. The novel findings of the current study are (1) *PRDM16* loss-of-function variants are sufficient to cause LVNC in humans in the absence of 1p36 deletion syndrome; (2) *PRDM16* loss-of-function variants are associated with impaired myocardium development, likely due to defective myocyte proliferation and differentiation, which results in severe LVNC, (3) PRDM16 bidirectionally regulates TGFβ signaling in a temporally-dependent manner; and (4) Prdm16 directly binds to the *Tgfb3* gene promoter and represses its expression in H9c2 rat cardiomyoblasts.

Using whole exome sequencing, we identified two *de novo* variants (Q187X and c.676+2T>C) in *PRDM16* in two unrelated pediatric patients presenting with LVNC by echocardiography and who did not have any alterations in genes previously known to cause LVNC or any other cardiomyopathy. These variants are novel, predicted by *in silico* analysis and current ACMG guidelines to be pathogenic, and have a mode of inheritance suggesting disease-association. Contrary to inherited forms of LVNC, the discovered variants in *PRDM16* that caused LVNC in this study demonstrate a *de novo* mode of inheritance, suggesting that loss-of-function variants in PRDM16 result in early-onset and severe cardiomyopathy which would preclude transmission of the disease allele to offspring. Our findings validate a recent associative study[21] linking *PRDM16* variants with LVNC in a meta-analysis of six different LVNC cohorts and suggest a causal role for *PRDM16* variants in the development of LVNC.

Proband 1 exhibited LVNC at 4 days with preserved function but quickly progressed to severe heart failure due to loss of systolic function and LV dilation. This represents a dilated cardiomyopathy (DCM)-like progression of LVNC known to occur in some patients with LVNC[1]. Conversely, proband 2 had LVNC with intact LV systolic function and no LV dilation at 5 years of age. This apparent divergency in cardiac performance is not completely understood but could be due to the nature of the variant (truncation versus splice variant), the gender of the proband, or the genetic landscape of each proband. This may represent a vulnerable myocardial substrate which is at risk of developing heart failure, although the variable expressivity of this locus, and of all forms of genetic cardiomyopathy, are not well understood.

This study generated the first model of a human *PRDM16* disease-associated variants and findings were paired with *Prdm16*$^{QX/WT}$ knock-in. Careful histologic examination of the LV in the *Prdm16*$^{QX/WT}$ knock-in mice may suggest a severe phenotype in the *Prdm16*$^{QX/QX}$ homozygous mice, with embryonic lethality secondary to LVNC with marked impairment of the development of the compact layer of the mouse heart. *Prdm16*$^{QX/WT}$ mice have a milder phenotype marked by underdevelopment of the ventricle and mild noncompaction. This gene dose-effect may be due to the maintenance of *Prdm16* mRNA expression, again suggesting that mice may require a complete loss of Prdm16 to exhibit LVNC while haplo-insufficient *PRDM16* loss in humans is sufficient to cause LVNC. Another possibility is that PRDM16 may regulate distinct developmental pathways relevant to LVNC development in humans, underscoring the necessity for studies in human cardiomyocytes such as iPSC-CMs. Interestingly, we see a sex-bias in survival among *Prdm16*$^{QX/WT}$ mice, with female mice having higher embryonic lethality rates, as we see more male mice born. These findings are in agreement with our recent work, identifying worse survival among female Prdm16 knockout mice compared to males as well as emerging evidence that females with *PRDM16* deleted in 1p36del syndrome have a higher chance of developing cardiomyopathy than males who also lack *PRDM16* in 1p36del syndrome[22]. Should this be found in other models of disease, it would suggest a sex-specific association between loss of *PRDM16* and the risk of developing cardiomyopathy, heart failure, and even mortality.

Our human *PRDM16* mutation-derived murine model is important as there have been several murine *Prdm16* knockout models that exhibited variable cardiac phenotypes. Global *Prdm16* knockout is embryonic lethal[12]; thus cardiac-specific knockouts have been generated. *Xmlc2-Cre* or *cTnT-Cre* driven *Prdm16* knockouts demonstrate LV-specific dilation and dysfunction, as well as biventricular non-compaction[14]. *Mesp1-Cre* driven knockouts demonstrate age-associated ventricular fibrosis and cardiac hypertrophy[13, 23]. Two *Myh6-Cre* driven knockouts have been generated and both demonstrate cardiac hypertrophy and early onset dilated cardiomyopathy[12, 16]. Consistent with these models, our *Prdm16*^{QX}/QX homozygous mice exhibited LV non-compaction and *Prdm16*^{QX}/WT heterozygous mice developed cardiac hypertrophy and fibrosis. These inconsistent phenotypes may be explained in part by the efficiency of the *Cre* driver to deplete *Prdm16* but can also suggest that Prdm16 may regulate distinct developmental genes in developmental stage-specific manner and may reflect background genetic features. These findings are consistent with the observation that humans with *PRDM16* variants in the presence of 1p36 deletion syndrome develop a spectrum of cardiac phenotypes including LVNC alone, DCM alone or both[10].

This study provides novel insights into the role of PRDM16 in TGFβ signaling. We demonstrate through RNA-seq and qPCR that PRDM16 regulates TGFB in a time-dependent manner. PRDM16 has been suggested as a negative regulator of canonical TGFβ signaling[12, 14]. Indeed, in 5-month-old *Myh6-Cre* driven *Prdm16* knockouts, TGFβ signaling was interrogated and observed to be elevated with hyperphosphorylated Smad2[12]. However, the relationship between TGFβ signaling and cardiomyopathy is complex. Given the known role of TGFB in cardiac fibrosis, Nam et. al inhibited the TGFB receptors at 2 months of age in *Myh6-Cre-Prdm16* KO mice. Interestingly, this strategy failed to rescue the fibrotic phenotype of these mice[12]. They suggest that TGFB is not responsible for cardiac

fibrosis in this model. Another possibility, as our data indicate, is that TGFB may have a dynamic transcriptional and regulatory time course.

These findings are consistent with literature reports of upregulation of TGFB in fetal cardiomyocyte differentiation[24] and TGFB promotion of embryonic trabecular cardiomyocyte proliferation[25], as well as seemingly opposite findings in adults demonstrating that TGFB expression in adult hearts is associated with fibrosis[13], hypertrophy[26], and adverse cardiac remodeling such as induction of fetal-type myosin heavy chain[27]. Recent transcriptomic analysis of cell-cycle regulation in cardiomyocytes over time (E10.5, P1, and 8-weeks-old) identified TGFβ signaling pathways as the most differentially regulated pathway[28]. Thus, TGFβ signaling appears dynamic and heterogenous depending on the specific ligand, receptor, and developmental stage. Importantly, this study presents evidence that TGFβ signaling is positively regulated by PRDM16 early in development then suppressed later in the mature mouse heart. These findings are of note as they demonstrate *PRDM16* variants are capable of generating TGFB-mediated effects that vary by time and conspire to disrupt normal myocardial development. Together with previously published findings, we propose loss of *PRDM16* leads to a lack of TGFB induction in early development and dysregulation and hyperactivity as the mouse heart matures according to our working mode[13, 18, 29, 30] (Fig 8).

This is particularly interesting given recent findings that suggest that *PRDM16* deletion-associated LVNC may result from loss of compact myocardial identity[14]. Consistent with this, Kodo et al. noted PRDM16 negatively regulates TGFβ signaling and suggest this axis may contribute to LVNC[19]. In this same work, they demonstrated that TGFB1 signaling is required for adequate proliferation of compacted myocardium and deficiency in TGFB1 signaling early caused LVNC[19]. Our study links these findings: PRDM16 induces TGFβ signaling early during mouse heart development and without it LVNC can develop, but later in cardiac maturation PRDM16 suppresses TGFβ signaling and maintains compact myocardial identity. Altogether, our results provide evidence that PRDM16 acts both as a positive and a negative regulator of TGFB that is temporally-variable. Lastly, we demonstrated mechanistically that Prdm16 binds both *Tgfb2* and *Tgfb3* gene promoters and differentially modulates H3K4 methylation marks in H9c2 rat cardiomyoblasts.

Limitations to this study include the possibility of genetic selection bias as probands presented with cardiomyopathy and were later found to have *PRDM16* mutations. It remains to be determined what the true prevalence of pathogenic *PRDM16* variants is and how penetrant the disease phenotype might be. We sought to mitigate this bias by searching for other putative cardiomyopathic mutations in these probands before concluding *PRDM16* was causative, as well as querying family members some of whom were asymptomatic. Further research might entail generation of a collaborative registry to compile cases of isolated *PRDM16* mutation for better clinical and molecular characterization. Other limitations to this study include the difficulty of predicting pathogenicity of splice-site variants, such as that of Proband 2. The degree to which these variants may disrupt mRNA is a future direction. Finally, we put forward a potential mechanism by which loss of *PRDM16* may result in LVNC through TGFβ signaling in a developmentally specific manner. We cannot exclude the possibly that other mechanisms may play an important, and parallel, role

in LVNC development. Additional work is needed to understand the complex underpinnings of both myocardial development and myopathic remodeling.

CONCLUSION/IMPLICATIONS FOR CLINICAL PRACTICE

PRDM16 has been implicated in cardiomyopathy through animal studies, associational studies, and clinical genetics work on 1p36 deletion syndrome. For the first time, this study examined isolated PRDM16 deficiency in human cells by identifying a proband with a loss-of-function variant in *PRDM16*. This variant was studied in both iPSC-CMs and mice and demonstrated that PRDM16 deficiency impairs cardiac proliferation and differentiation resulting in LVNC. The current and the previous studies shed light on the possible mechanisms underlying the multitude clinical phenotypes observed in humans with *PRDM16* mutations, as well as the pathogenesis of LVNC. Further, this study developed valuable tools (iPSC-CMs with *PRDM16* variants and Prdm16$^{Q187X/WT}$ knock-in mice) that may help study and test potential therapies to restore cardiac defects in humans.

Supplementary Material

Refer to Web version on PubMed Central for supplementary material.

Acknowledgments

We gratefully acknowledge the support of the patients and families who have graciously accepted to participate in this study. We acknowledge Mr. Chris Stubben at the University of Utah Bioinformatics core for analyzing the RNA-seq. We acknowledge Mrs. Diana Lim, a Graphics Specialist in the Molecular Medicine Program at the University of Utah, for her support in preparing the figures presented in this manuscript.

Sources of Funding

This work is supported by the National Heart, Lung and Blood Institute (NHLBI) grant R01HL149870-01A1 to S.B. R. R.G. is supported by American Heart Association Career Development Award. RJK is supported by the Sarnoff Cardiovascular Research Foundation. R.M.P. is supported by American Heart Association Predoctoral Fellowship 829638. K.D. is supported by American Heart Association PRE35120356. M.W.S. is supported by F32HL144034. E.C. is supported by NIH Ruth L. Kirschstein National Research Service Award (NRS) institutional training grant T35DK103596. T.A.W. is supported by National Heart, Lung and Blood Institute (NHLBI) grant T32HL139430. X.H.T.W. is supported by NHLBI R01HL089598, R01HL147108, and R01HL153350. S.F. is supported by Nora Eccles Harrison Treadwell Foundation Grant 10038331. A.P.L. is supported by NHLBI K08-HL136839, R01-HL160654, Doris Duke Charitable Foundation (CSDA-2020098), John Taylor Babbitt Foundation, The Hartwell Foundation, Additional Ventures, Y.T. and Alice Chen Pediatric Genetics and Genomics Research Center. M.W. is supported by NHLBI R01HL121700-06A1 and AHA 20TPA35490051.

NON-STANDARD ABBREVIATIONS and ACRONYMS

CADD	combined annotation dependent depletion
c.676+2T>C	NM_022114.4 (PRDM16): c.676+2T>C
ChIP	chromatin immunoprecipitation
CRISPR-Cas9	clustered regularly interspaced short palindromic repeats and CRISPR-associated protein 9
DCM	dilated cardiomyopathy

DANN	deep neural network
EdU	5-Ethynyl-2’-deoxyuridine
HEK293T-EV	HEK293T empty vector
hPRDM16-WT	human PRDM16 wild-type
hPRDM16-QX	human PRDM16-Q187X
iPSCs	induced pluripotent stem cells
iPSC-CMs	induced pluripotent stem cell-derived cardiomyocytes
KEGG	Kyoto Encyclopedia of Genes and Genomes
LV	left ventricular
LVDd	left ventricular end diastolic dimension
LVDs	left ventricular end systolic dimension
LVEDV	left ventricular end diastolic volume
LVESV	left ventricular end systolic volume
LVNC	left ventricular noncompaction cardiomyopathy
NCBI	National Center for Biotechnology Information
NRVMs	neonatal rat cardiomyocytes
PW	posterior wall
Q187X	PRDM16-Q187X
SD	standard deviation
SVT	supraventricular tachycardia
TGFβ	transforming growth factor-β
WGA	wheat germ agglutinin
WT	wild type

Reference:

1. Towbin JA, Lorts A, and Jefferies JL, Left ventricular non-compaction cardiomyopathy. Lancet, 2015. 386(9995): p. 813–25. [PubMed: 25865865]
2. Greutmann M, et al. , Predictors of adverse outcome in adolescents and adults with isolated left ventricular noncompaction. Am J Cardiol, 2012. 109(2): p. 276–81. [PubMed: 22036106]
3. Klaassen S, et al. , Mutations in sarcomere protein genes in left ventricular noncompaction. Circulation, 2008. 117(22): p. 2893–901. [PubMed: 18506004]
4. Lipshultz SE, et al. , Pediatric cardiomyopathies: causes, epidemiology, clinical course, preventive strategies and therapies. Future Cardiol, 2013. 9(6): p. 817–48. [PubMed: 24180540]

5. Ware SM, et al. , Genetic Causes of Cardiomyopathy in Children: First Results From the Pediatric Cardiomyopathy Genes Study. J Am Heart Assoc, 2021. 10(9): p. e017731. [PubMed: 33906374]
6. Ouellette AC, et al. , Clinical genetic testing in pediatric cardiomyopathy: Is bigger better? Clin Genet, 2018. 93(1): p. 33–40. [PubMed: 28369760]
7. Parker LE and Landstrom AP, The clinical utility of pediatric cardiomyopathy genetic testing: From diagnosis to a precision medicine-based approach to care. Prog Pediatr Cardiol, 2021. 62: p. 101413. [PubMed: 34776723]
8. Jang S, et al. , 1p36 Deletion Syndrome and Left Ventricular Non-compaction Cardiomyopathy-Two Cases Report. Front Pediatr, 2021. 9: p. 653633. [PubMed: 34164357]
9. Shimada IS, et al. , Prdm16 is required for the maintenance of neural stem cells in the postnatal forebrain and their differentiation into ependymal cells. Genes Dev, 2017. 31(11): p. 1134–1146. [PubMed: 28698301]
10. Arndt AK, et al. , Fine mapping of the 1p36 deletion syndrome identifies mutation of PRDM16 as a cause of cardiomyopathy. Am J Hum Genet, 2013. 93(1): p. 67–77. [PubMed: 23768516]
11. de Leeuw N and Houge G, Loss of PRDM16 is unlikely to cause cardiomyopathy in 1p36 deletion syndrome. Am J Hum Genet, 2014. 94(1): p. 153–4. [PubMed: 24387995]
12. Nam JM, et al. , Cardiac-specific inactivation of Prdm16 effects cardiac conduction abnormalities and cardiomyopathy-associated phenotypes. Am J Physiol Heart Circ Physiol, 2020. 318(4): p. H764–H777. [PubMed: 32083975]
13. Cibi DM, et al. , Prdm16 Deficiency Leads to Age-Dependent Cardiac Hypertrophy, Adverse Remodeling, Mitochondrial Dysfunction, and Heart Failure. Cell Rep, 2020. 33(3): p. 108288. [PubMed: 33086060]
14. Wu T, et al. , PRDM16 Is a Compact Myocardium-Enriched Transcription Factor Required to Maintain Compact Myocardial Cardiomyocyte Identity in Left Ventricle. Circulation, 2022. 145(8): p. 586–602. [PubMed: 34915728]
15. Pires KM BS, Abstract 100: PRDM16 is a Novel Regulator of Cardiac Hypertrophy, Remodeling and Mitochondrial Dynamics. Circ Res, 2018. 123: A100.
16. Kang JO, et al. , A cardiac-null mutation of Prdm16 causes hypotension in mice with cardiac hypertrophy via increased nitric oxide synthase 1. PLoS One, 2022. 17(7): p. e0267938. [PubMed: 35862303]
17. Shull LC, et al. , PRDM paralogs antagonistically balance Wnt/beta-catenin activity during craniofacial chondrocyte differentiation. Development, 2022. 149(4): p. 200082.
18. Bjork BC, et al. , Prdm16 is required for normal palatogenesis in mice. Hum Mol Genet, 2010. 19(5): p. 774–89. [PubMed: 20007998]
19. Kodo K, et al. , iPSC-derived cardiomyocytes reveal abnormal TGF-beta signalling in left ventricular non-compaction cardiomyopathy. Nat Cell Biol, 2016. 18(10): p. 1031–42. [PubMed: 27642787]
20. Chi J and Cohen P, The Multifaceted Roles of PRDM16: Adipose Biology and Beyond. Trends Endocrinol Metab, 2016. 27(1): p. 11–23. [PubMed: 26688472]
21. Mazzarotto F, et al. , Systematic large-scale assessment of the genetic architecture of left ventricular noncompaction reveals diverse etiologies. Genet Med, 2021. 23(5): p. 856–864. [PubMed: 33500567]
22. Kramer RJ, et al. , PRDM16 deletion is associated with sex-dependent cardiomyopathy & cardiac mortality: A translational, multi-institutional cohort study. Circ Genom Precis Med, 2023. 16: p. 390–400. [PubMed: 37395136]
23. Pesce M, et al. , Cardiac fibroblasts and mechanosensation in heart development, health and disease. Nat Rev Cardiol, 2023. 20(5): p. 309–324. [PubMed: 36376437]
24. Dickson MC, et al. , RNA and protein localisations of TGF beta 2 in the early mouse embryo suggest an involvement in cardiac development. Development, 1993. 117(2): p. 625–39. [PubMed: 7687212]
25. Uribe V, et al. , In vivo analysis of cardiomyocyte proliferation during trabeculation. Development, 2018. 145(14): p. 164194.
26. Li RK, et al. , Natural history of fetal rat cardiomyocytes transplanted into adult rat myocardial scar tissue. Circulation, 1997. 96(9 Suppl): p. II-179–86; discussion 186–7.

27. Parker D, et al. , Practice nurse involvement in the management of adults with type 2 diabetes mellitus attending a general practice: results from a systematic review. Int J Evid Based Healthc, 2016. 14(2): p. 41–52. [PubMed: 27077334]
28. Mohamed TMA, et al. , Regulation of Cell Cycle to Stimulate Adult Cardiomyocyte Proliferation and Cardiac Regeneration. Cell, 2018. 173(1): p. 104–116 e12. [PubMed: 29502971]
29. Sorensen DW and van Berlo JH, The Role of TGF-beta Signaling in Cardiomyocyte Proliferation. Curr Heart Fail Rep, 2020. 17(5): p. 225–233. [PubMed: 32686010]
30. Leone M, Magadum A, and Engel FB, Cardiomyocyte proliferation in cardiac development and regeneration: a guide to methodologies and interpretations. Am J Physiol Heart Circ Physiol, 2015. 309(8): p. H1237–50. [PubMed: 26342071]
31. Ishchenko Y, et al. , Selective Calcium-Dependent Inhibition of ATP-Gated P2X3 Receptors by Bisphosphonate-Induced Endogenous ATP Analog ApppI. J Pharmacol Exp Ther, 2017. 361(3): p. 472–481. [PubMed: 28404687]
32. Karczewski KJ, et al. , The mutational constraint spectrum quantified from variation in 141,456 humans. Nature, 2020. 581(7809): p. 434–443. [PubMed: 32461654]
33. Richards S, et al. , Standards and guidelines for the interpretation of sequence variants: a joint consensus recommendation of the American College of Medical Genetics and Genomics and the Association for Molecular Pathology. Genet Med, 2015. 17(5): p. 405–24. [PubMed: 25741868]
34. Landrum MJ, et al. , ClinVar: improving access to variant interpretations and supporting evidence. Nucleic Acids Res, 2018. 46(D1): p. D1062–D1067. [PubMed: 29165669]
35. Choi Y, et al. , Predicting the functional effect of amino acid substitutions and indels. PLoS One, 2012. 7(10): p. e46688. [PubMed: 23056405]
36. Corpet F, Multiple sequence alignment with hierarchical clustering. Nucleic Acids Res, 1988. 16(22): p. 10881–90. [PubMed: 2849754]
37. Rentzsch P, et al. , CADD: predicting the deleteriousness of variants throughout the human genome. Nucleic Acids Res, 2019. 47(D1): p. D886–D894. [PubMed: 30371827]
38. Quang D, Chen Y, and Xie X, DANN: a deep learning approach for annotating the pathogenicity of genetic variants. Bioinformatics, 2015. 31(5): p. 761–3. [PubMed: 25338716]
39. Feng BJ, PERCH: A Unified Framework for Disease Gene Prioritization. Hum Mutat, 2017. 38(3): p. 243–251. [PubMed: 27995669]
40. Richardson CD, et al. , Enhancing homology-directed genome editing by catalytically active and inactive CRISPR-Cas9 using asymmetric donor DNA. Nat Biotechnol, 2016. 34(3): p. 339–44. [PubMed: 26789497]
41. Paredes L, et al. , What happens with organic micropollutants during UV disinfection in WWTPs? A global perspective from laboratory to full-scale. J Hazard Mater, 2018. 342: p. 670–678. [PubMed: 28898864]
42. Hodgkins A, et al. , WGE: a CRISPR database for genome engineering. Bioinformatics, 2015. 31(18): p. 3078–80. [PubMed: 25979474]
43. Bolli R, New Initiatives to Improve the Rigor and Reproducibility of Articles Published in Circulation Research. Circ Res, 2017. 121(5): p. 472–479. [PubMed: 28819032]
44. Ginsburg GS, Shah SH, and McCarthy JJ, Taking cardiovascular genetic association studies to the next level. J Am Coll Cardiol, 2007. 50(10): p. 930–2. [PubMed: 17765118]
45. Esposito G, et al. , Cellular and functional defects in a mouse model of heart failure. Am J Physiol Heart Circ Physiol, 2000. 279(6): p. H3101–12. [PubMed: 11087268]
46. Chen G, et al. , Chemically defined conditions for human iPSC derivation and culture. Nat Methods, 2011. 8(5): p. 424–9. [PubMed: 21478862]
47. Battaglia RA, et al. , Site-specific phosphorylation and caspase cleavage of GFAP are new markers of Alexander disease severity. Elife, 2019. 8: p. 47789.
48. Molina SG, Beltran AA, and Beltran AS, Generation of an integration-free induced pluripotent stem cell line (UNC001-A) from blood of a healthy individual. Stem Cell Res, 2020. 49: p. 102015. [PubMed: 33038744]
49. Dobaczewski M, Chen W, and Frangogiannis NG, Transforming growth factor (TGF)-beta signaling in cardiac remodeling. J Mol Cell Cardiol, 2011. 51(4): p. 600–6. [PubMed: 21059352]

50. Burridge PW, et al. , Chemically defined generation of human cardiomyocytes. Nat Methods, 2014. 11(8): p. 855–60. [PubMed: 24930130]

51. Musunuru K, et al. , Induced Pluripotent Stem Cells for Cardiovascular Disease Modeling and Precision Medicine: A Scientific Statement From the American Heart Association. Circ Genom Precis Med, 2018. 11(1): p. e000043. [PubMed: 29874173]

52. Love MI, Huber W, and Anders S, Moderated estimation of fold change and dispersion for RNA-seq data with DESeq2. Genome Biol, 2014. 15(12): p. 550. [PubMed: 25516281]

53. Huber W, et al. , Orchestrating high-throughput genomic analysis with Bioconductor. Nat Methods, 2015. 12(2): p. 115–21. [PubMed: 25633503]

54. Mootha VK, et al. , PGC-1alpha-responsive genes involved in oxidative phosphorylation are coordinately downregulated in human diabetes. Nat Genet, 2003. 34(3): p. 267–73. [PubMed: 12808457]

55. Miao L, et al. , The Spatiotemporal Expression of Notch1 and Numb and Their Functional Interaction during Cardiac Morphogenesis. Cells, 2021. 10(9): p. 2192. [PubMed: 34571841]

56. Zhao C, et al. , Numb family proteins are essential for cardiac morphogenesis and progenitor differentiation. Development, 2014. 141(2): p. 281–95. [PubMed: 24335256]

57. Warren JS, et al. , Histone methyltransferase Smyd1 regulates mitochondrial energetics in the heart. Proc Natl Acad Sci U S A, 2018. 115(33): p. E7871–E7880. [PubMed: 30061404]

What is New?

- The *PRDM16-Q187X* nonsense variant causes non-compaction cardiomyopathy in humans and mice.
- Nonsense variant in *PRDM16* altered TGFB signaling in human induced pluripotent stem cells-derived cardiomyocytes and in mouse heart.

What are the Clinical Implications?

- Loss-of-function mutations in *PRDM16* are associated with non-compaction cardiomyopathy with pediatric onset heart failure.
- PRDM16-associated non-compaction cardiomyopathy results from alteration in TGFβ signaling which may be a potential therapeutic target for treating this development defect.

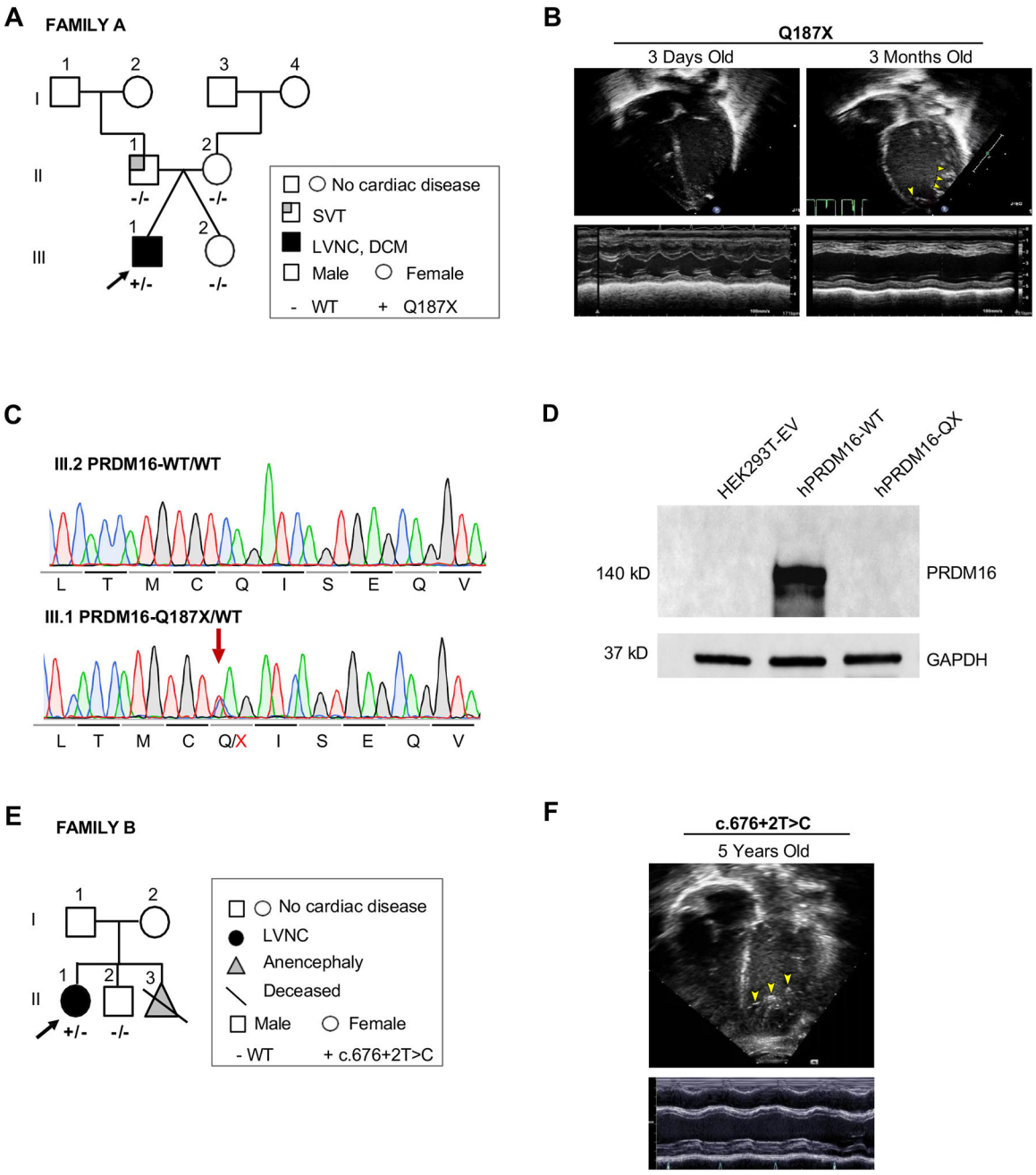

Figure 1:

Loss-of-function genetics variants in *PRDM16* are associated with left ventricular noncompaction cardiomyopathy (LVNC). (**a**) Schematic pedigree of Family A with LVNC. Proband 1 (III.1, arrow) hosts a heterozygous nonsense mutation (PRDM16-Q187X) denoted with a + and has LVNC with pediatric onset heart failure. DCM, dilated cardiomyopathy. SVT, supraventricular tachycardia. (**b**) Echocardiogram of Proband 1 demonstrates trabeculations of the left ventricular apex consistent with LVNC (yellow arrowheads) present at 3 days of life that progressed to DCM by 3 months of age. (**c**) Sequence chromatogram of genotype wild-type III.2 and genotype PRDM16-Q187X III.1

kindred with the mutated nucleotide noted with the arrow. (**d**) Western blot of empty vector (EV), human PRDM16 wild-type (WT), and PRDM16-Q187X protein (QX) overexpressed in HEK293T cells. (**e**) Schematic pedigree Family B with LVNC. Proband 2 (II.1, arrow) hosts a heterozygous splice variant (c.676+2T) in *PRDM16*. (**f**) Echocardiogram of Proband 2 (II.1) showing prominent apical trabeculations (yellow arrowheads) consistent with LVNC.

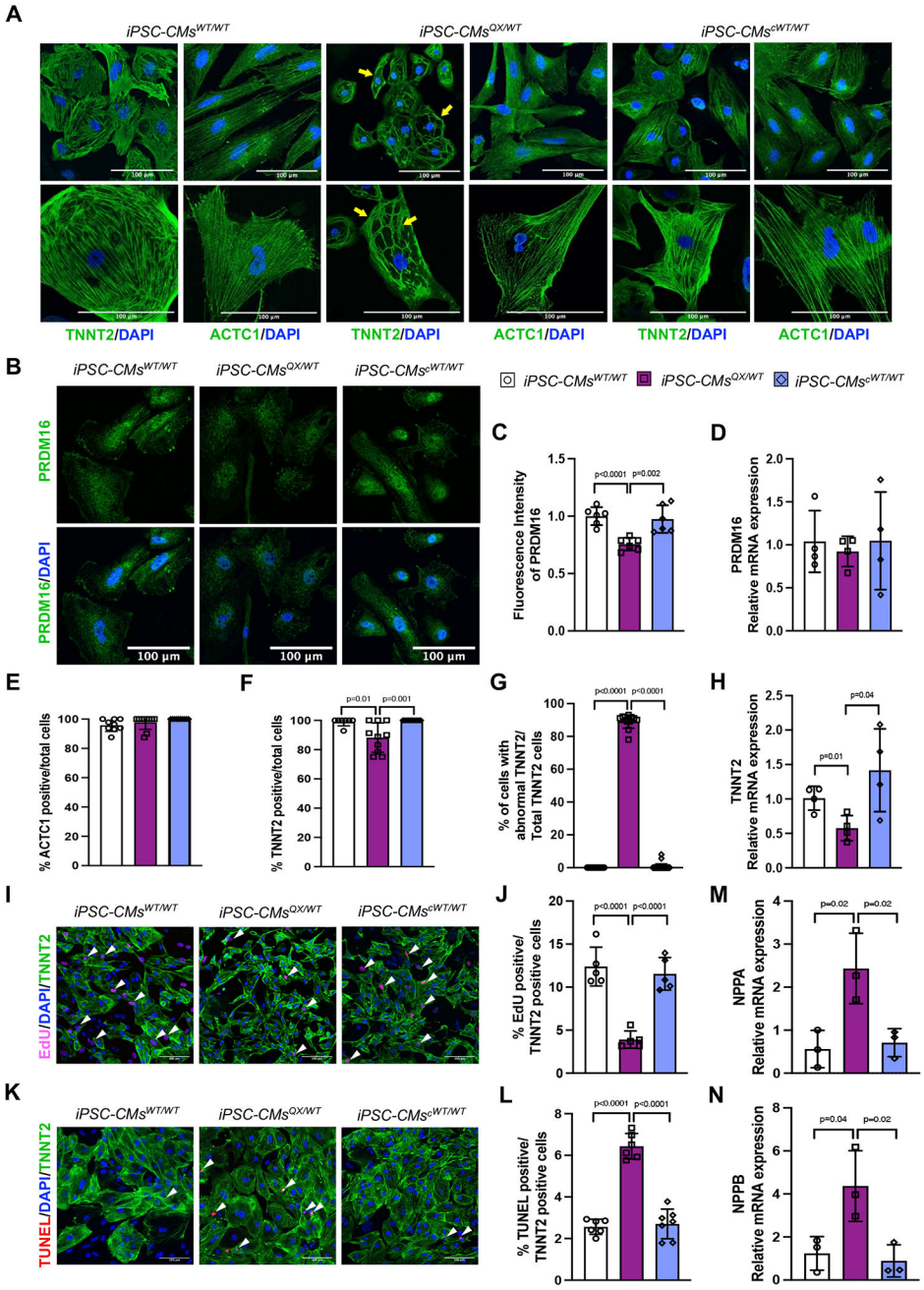

Figure 2:

PRDM16-Q187X impairs proliferation and increases apoptosis in iPSC-derived cardiomyocytes (iPSC-CMs). (**a**) Representative images of iPSC-CM differentiation markers Troponin T (TNNT2) and cardiac muscle alpha actin (ACTC1) in iPSC-CMs from non-isogenic control (iPSC-CMs$^{WT/WT}$), Proband 1 (iPSC-CMs$^{QX/WT}$) and CRISPR-corrected isogenic control (iPSC-CMs$^{cWT/WT}$). Yellow arrowheads demonstrated an abnormal organization of TNNT2 with loss of parallel myofilament alignment. (**b**) Immunostaining of nuclei (blue) and PRDM16 (green) in iPSC-CMs. (**c**) Fluorescence intensity of PRDM16 in iPSC-CMs (n=3). (**d**) PRDM16 mRNA expression in Proband 1 (iPSC-CMs$^{QX/WT}$)

compared with controls (n=4). (**e**) Quantification of ACTC1 expression in iPSC-CMs (n=3). (**f**) Quantification of TNNT2 expression in iPSC-CMs (n=3). (**g**) Quantification of cells with abnormal TNNT2 pattern over the total number of cells (n=3). (**h**) Relative mRNA expression (normalized to *RPL32*) of TNNT2 from iPSC-CMs (n=4). (**i**) Immunostaining of nuclei (blue), TNNT2 (green) and EdU (pink) in iPSC-CMs at 4 weeks. White arrowheads represent EdU positive cells. (**j**) Percentage of EdU positive cardiomyocytes in Proband 1 and controls (n=3). (**k**) Immunostaining of nuclei (blue), TNNT2 (green) and TUNEL (red) in iPSC-CMs at 4 weeks. White arrowheads represent TUNEL positive cells. (**l**) Percentage of TUNEL iPSC-CMs (n=3). (**m, n**) mRNA expression of *NPPA* (encoding natriuretic peptide A) and *NPPB* (encoding natriuretic peptide B) in iPSC-CMs (n=3). The bar graphs show the mean and error bars represent ± SD. Scale bar: 100 μm. P values generated using unpaired t-test.

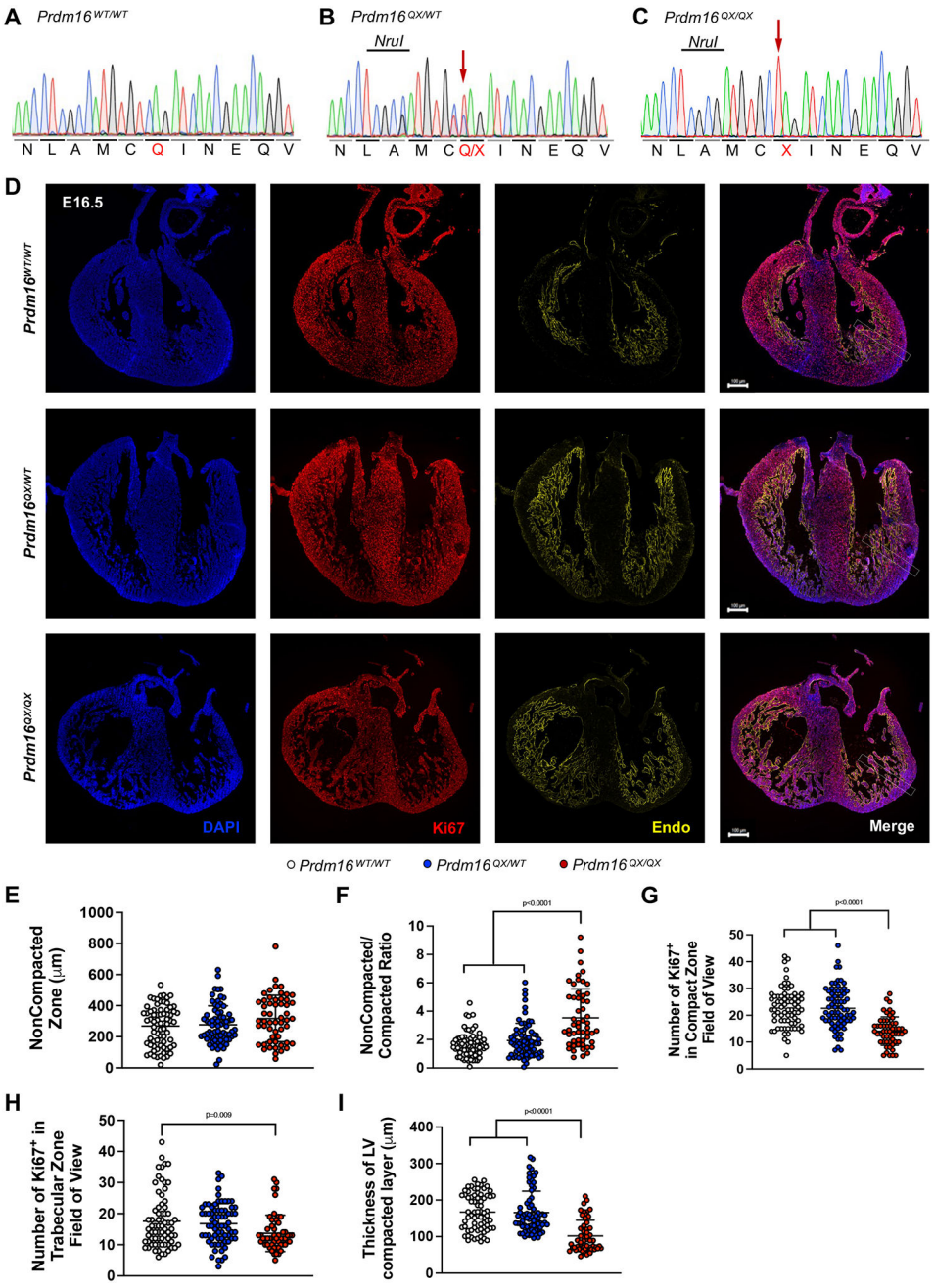

Figure 3:

Prdm16$^{QX/QX}$ homozygous mice display left ventricular compaction defect: (**a-c**) Sequence chromatograms confirming the genotype of control (*Prdm16*$^{WT/WT}$), heterozygote (*Prdm16*$^{QX/WT}$) and homozygous mutant (*Prdm16*$^{QX/QX}$) knock-in mice, respectively. *NruI*, Bsp68I restriction enzyme. (**d**) *Prdm16*$^{WT/WT}$, *Prdm16*$^{WT/QX}$ and *Prdm16*$^{QX/QX}$ E16.5 hearts were stained with endomucin (Endo) to label endocardial cell and Ki67 to identify proliferative cells. (**e-f**) Quantification of the thickness of noncompacted zone and the noncompacted/compacted ratio (at least three hearts per genotype, 6 fields were measured per section). (**g-h**) Cardiomyocyte proliferation rate using average of Ki67^{+} cells in six field

of view (at least three hearts per genotype). (**i**) Quantification of left ventricle thickness (at least three hearts per genotype, 6 different spots were measured per section). The bar graphs show the mean and error bars represent ± SD. Scale bars:100 μm. P-values generated using one-way ANOVA (not shown) followed by Tukey post hoc test.

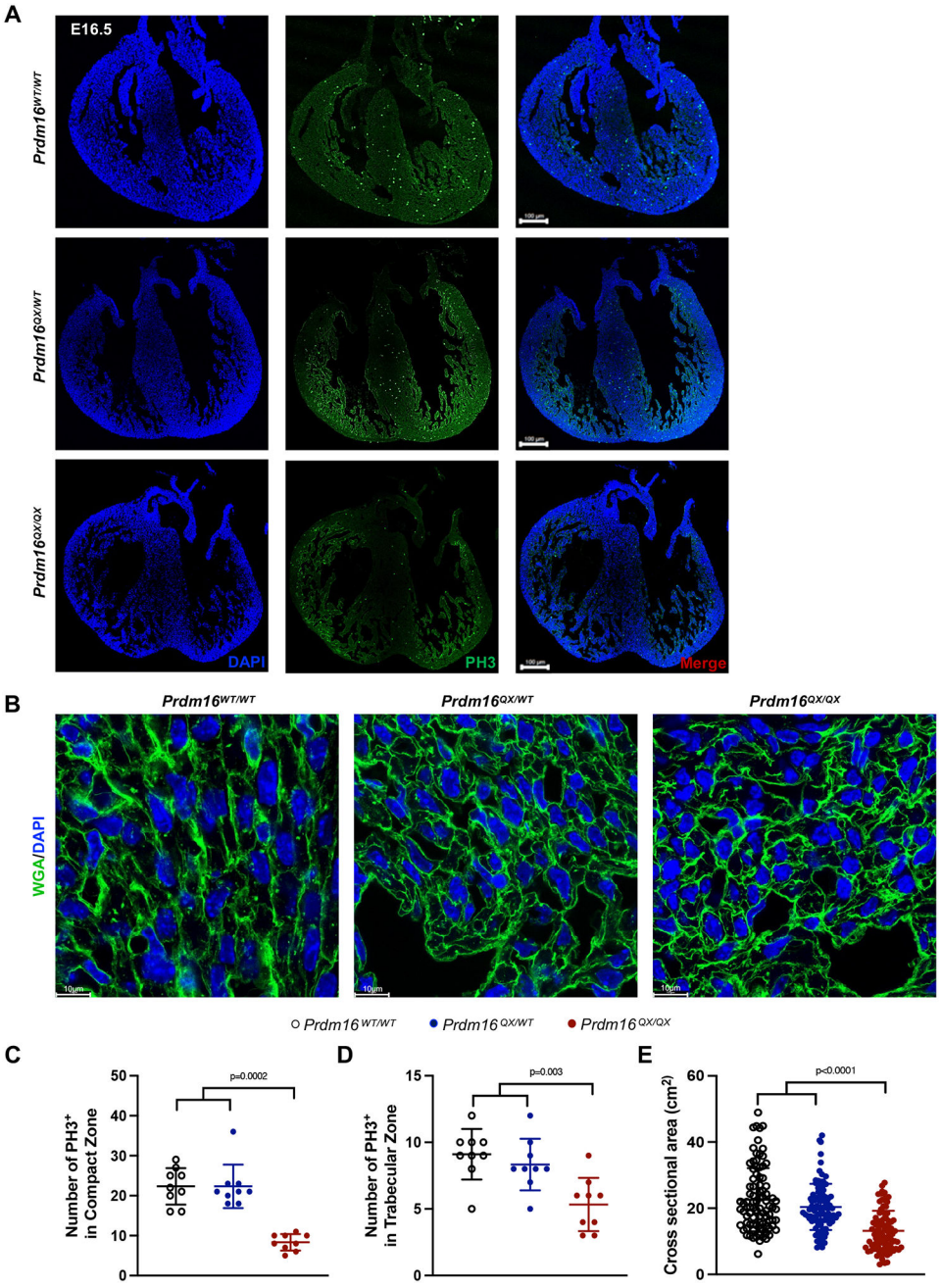

Figure 4:

Prdm16$^{QX/QX}$ homozygous mice display defects in cardiomyocyte development. (a) *Prdm16*$^{WT/WT}$, *Prdm16*$^{WT/QX}$, *Prdm16*$^{QX/QX}$ E16.5 hearts were stained with anti-histone H3 (PH3) to quantify proliferative cells. Scale bars:100 μm. (b) Representative WGA (Wheat germ agglutinin) staining images for visualizing cell size. Scale bars: 10um. (c, d) Quantification of PH3 positive (pH3^{+}) cells in both compact and trabecular areas of the heart show a significant decrease in cardiomyocyte proliferation rate in *Prdm16*$^{QX/QX}$ when compared to *Prdm16*$^{WT/WT}$, *Prdm16*$^{QX/WT}$ (calculated from at least 3 sections). (e) Quantification of cross-sectional area shows a significant decrease in

cell size in *Prdm16*$^{QX/QX}$ compared to *Prdm16*$^{WT/WT}$, *Prdm16*$^{QX/WT}$ (n=3 sections, 90 cardiomyocytes/section/group). The bar graphs show the mean and error bars represent ± SD. P-values generated using one-way ANOVA (not shown) followed by Tukey post hoc test.

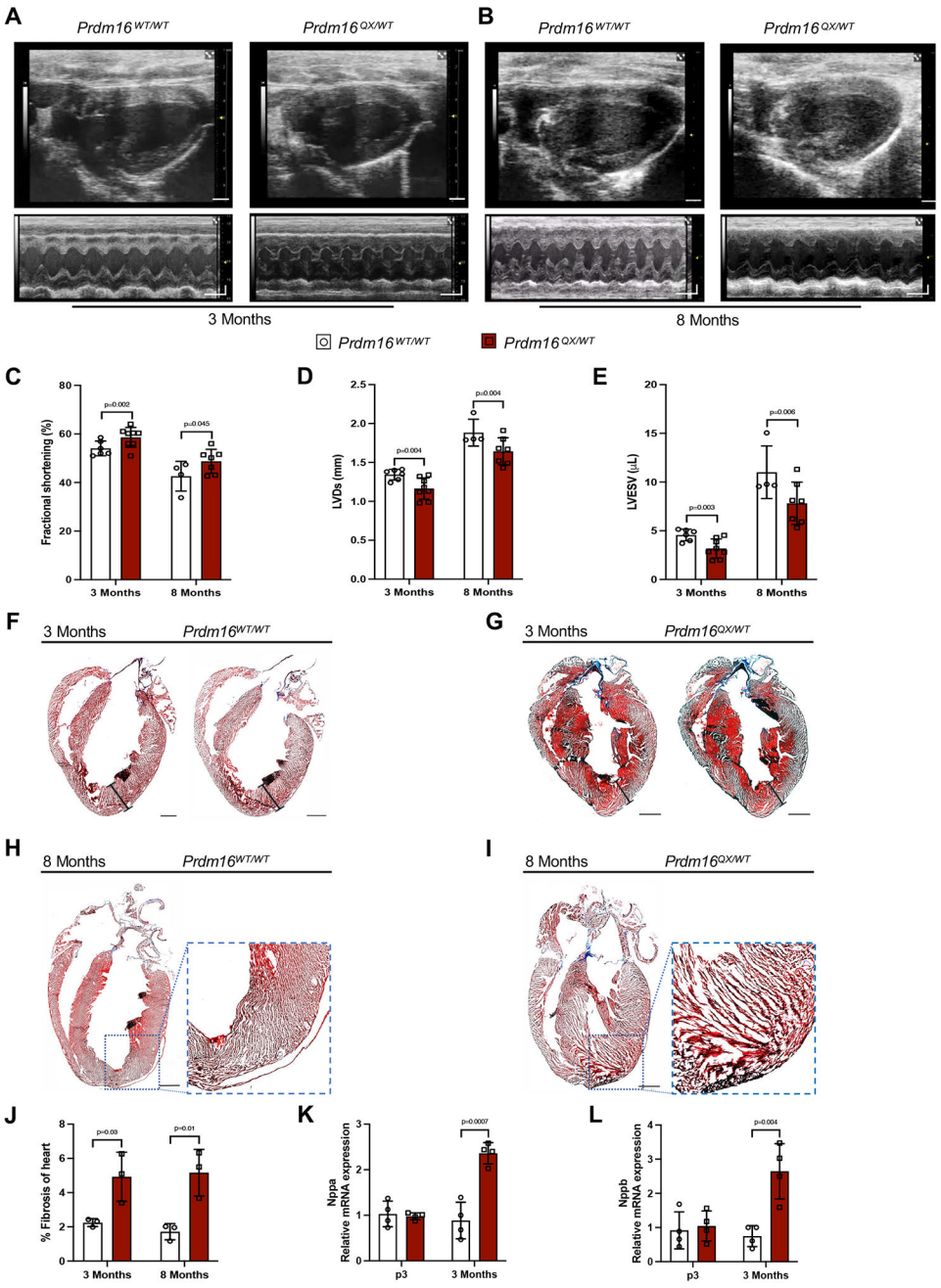

Figure 5:

Prdm16$^{QX/WT}$ mutant mice develop pathological cardiac remodeling. (**a, b**) Long-axis B-mode and M-mode echocardiographic images at 3 and 8 months, respectively. Scale bar:100 ms. (**c**) Ejection fraction (n=4, 6, 7 and 8 mice per group, each dot corresponds to a mouse); (**d**) Left ventricular diameter in systole (LVDs) (n=4, 6, 7 and 8 mice per group, each dot corresponds to a mouse); (**e**) Left ventricular end systolic volume (LVESV) in *Prdm16*$^{WT/WT}$ and *Prdm16*$^{QX/WT}$ mice at 3 and 8 months of age (n=4, 6, 7 and 8 mice per group, each dot corresponds to a mouse); (**f-i**) Histological analysis of heart sections stained with hematoxylin and eosin or trichrome from 3 and 8 months-old mice showing small

left ventricular (LV) size and internal dimensions. Scale bars: 1000 μm. (**j**) Quantification of the amount of fibrosis in the heart at 3 and 8 months, respectively (n=3 hearts). (**k, l**) Quantification of mRNA expression of *Nppa* (encoding natriuretic peptide A) and *Nppb* (encoding natriuretic peptide B) in hearts of 3 days (p3) and 3 months-old mice (n=4 hearts). The bar graphs show the mean and error bars represent ± SD. Comparisons are by unpaired t-tests.

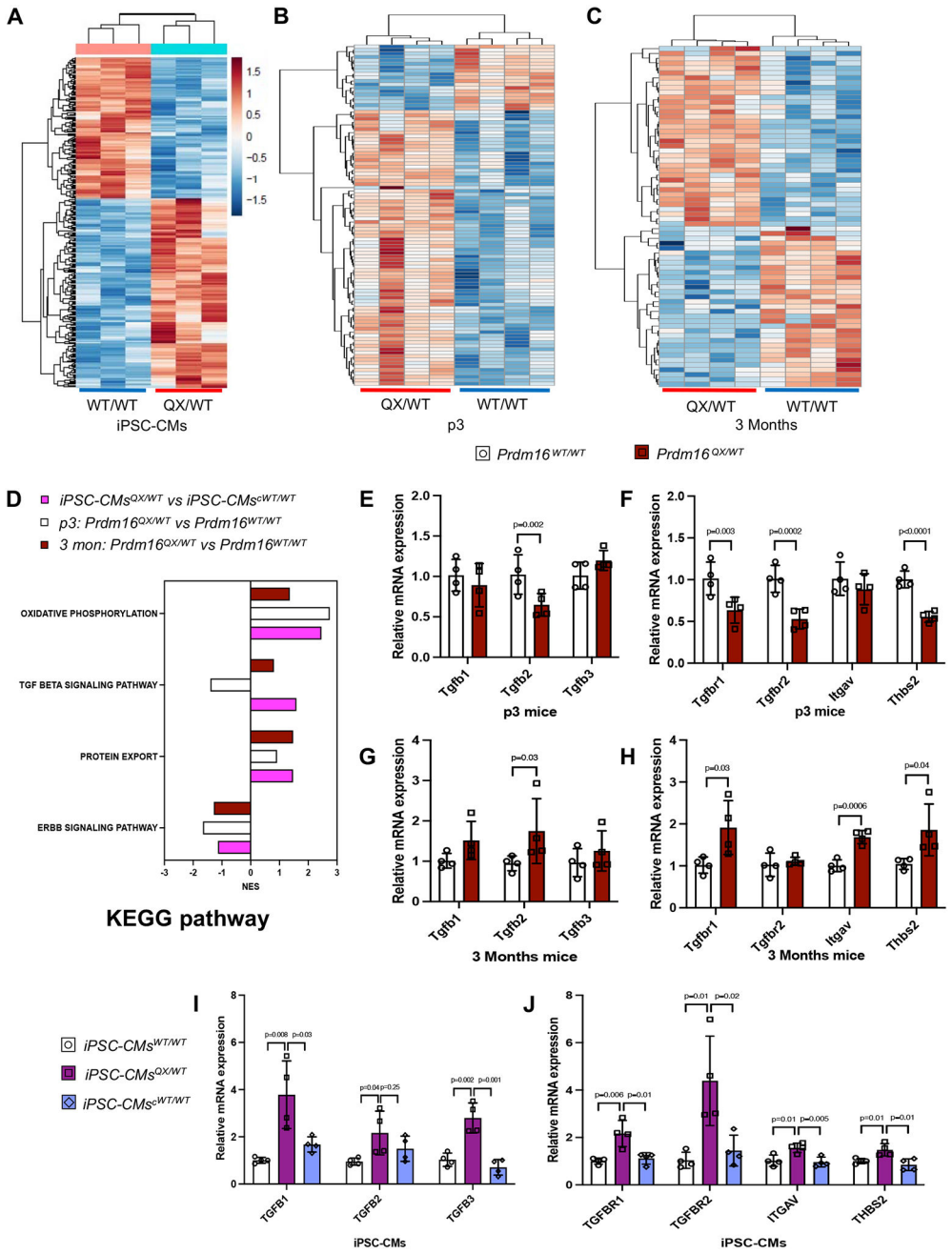

Figure 6:

PRDM16-Q187X is associated with modulation of developmentally-dependent *Tgfβ* signaling. (**a**) Heatmap of differentially expressed transcripts from RNA-seq analysis of mutant iPSC-cardiac myocytes (iPSC-CMs$^{QX/WT}$) and non-isogenic control (iPSC-CMs$^{WT/WT}$). (**b, c**) Heatmap representation of differentially expressed transcripts identified from RNA-seq analysis of 3 days (p3) and 3 months old control and Prdm16-Q187X mouse hearts. (**d**) Kyoto Encyclopedia of Genes and Genomes (KEGG) analysis of upregulated and downregulated pathways iPSC-CMs$^{QX/WT}$ vs iPSC-CMs$^{cWT/WT}$ as well as in hearts from 3 days (p3) and 3 months (3 mon) *Prdm16$^{WT/WT}$* and *Prdm16$^{QX/WT}$*, respectively.

(**e-h**) QRT-PCR validation of *Tgfβ* signaling from RNA-seq analysis of p3 and 3 months control *Prdm16*$^{QX/WT}$ (n=4). (**i, j**) QRT-PCR analysis showed significant increase in TGFβ signaling and downstream target genes mRNA expression in iPSC-CMs$^{QX/WT}$ compared to both iPSC-CMs$^{WT/WT}$ and isogenic iPSC-CMs$^{cWT/WT}$ at 4 weeks (n=4). The bar graphs show the mean and error bars represent ± SD. P-values generated using unpaired t-tests.

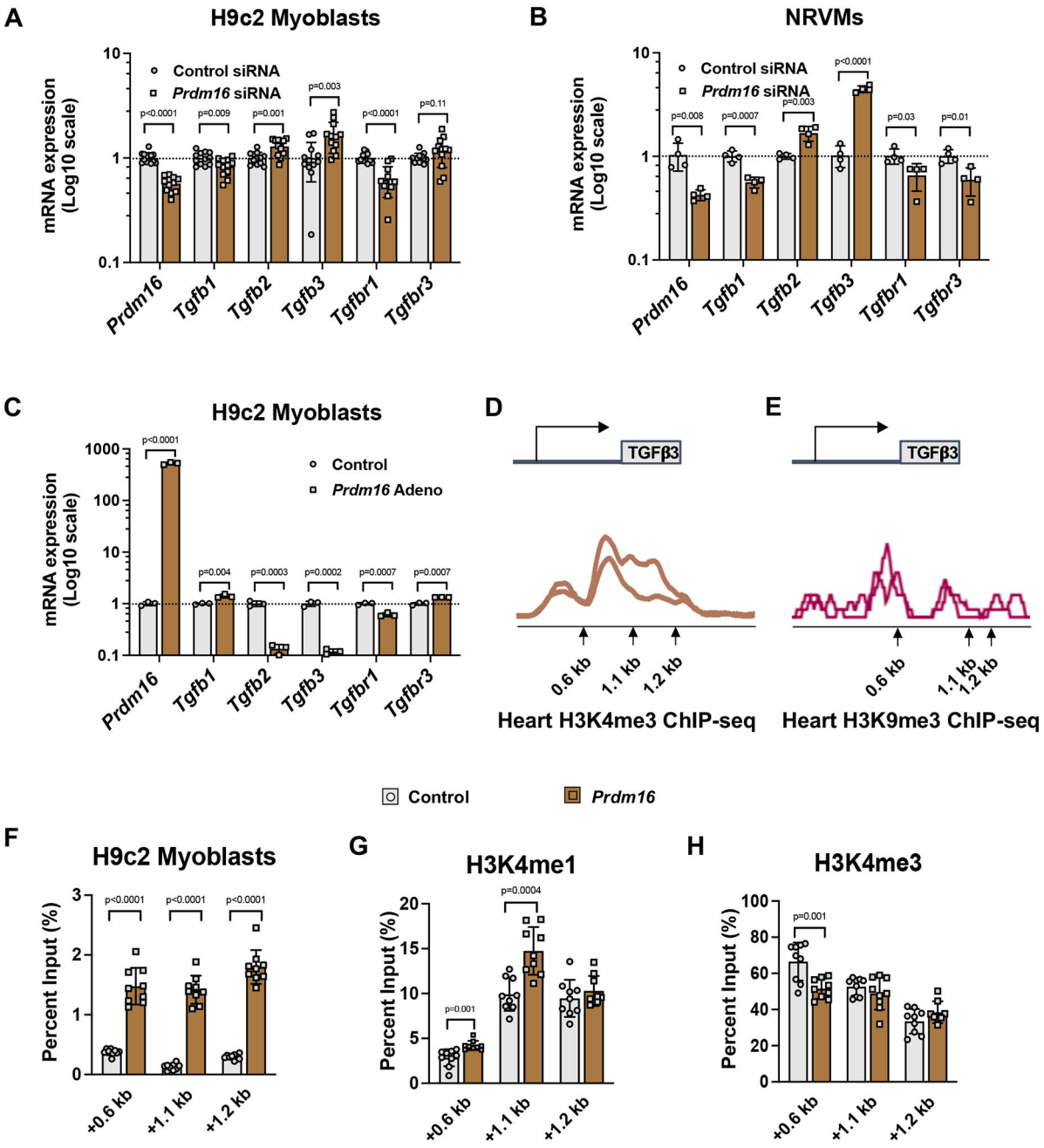

Figure 7:

Prdm16 regulates Tgfb gene transcription in cardiac cells. (**a**) mRNA expression of *Tgfb* genes in undifferentiated H9c2 rat cardiac myoblasts with Prdm16 siRNA knockdown or control siRNA (n=12). (**b**) mRNA expression of *Tgfb* genes in neonatal rat cardiomyocytes (NRVMs) with *Prdm16* siRNA or control siRNA (n=4). (**c**) mRNA expression of *Tgfb* genes in undifferentiated H9c2 cardiac myoblasts overexpressing *Prdm16* (n=3). (**d, e**) Previous ChIP-seq studies have established enrichment of H3K4me3 and H3K9me3 within the promoter regions of *Tgfb3* (WashU EpiGenome Database). (**f**) Prdm16 binding to the *Tgfb3* promoter region in H9c2 cardiac myoblast expressing Myc-tagged Prdm16 adenovirus or

not. ChIP-PCR negative control showing that PRDM16 is enriched at neither random intergenic region nor *Tbp* control gene (n=8). (**g**, **h**) Enrichment of histone H3K4me1 and reduced histone H3K4me3 methylation marks in the *Tgfb3* promoter region with Prdm16 over-expression in H9c2 myoblasts (n=8). The bar graphs show the mean and error bars represent ± SD. P-values generated using unpaired t-tests.

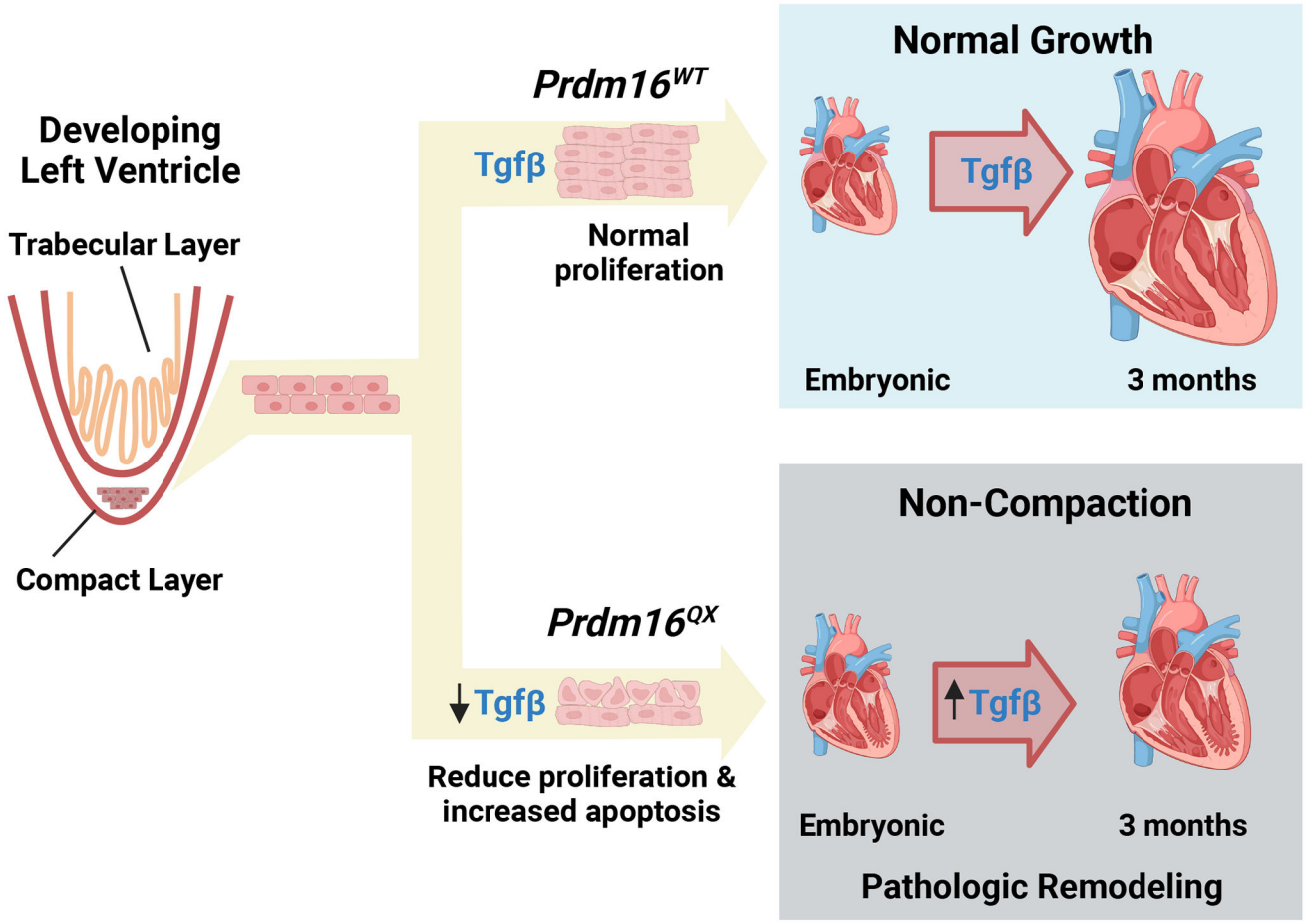

Figure 8:

A schematic of the proposed mechanism of PRDM16-mediated cardiomyopathy development. The PRDM16-Q187X variants results on impaired development of the compact layer of the left ventricle (LV) during fetal development in the setting of reduced TGFβ signaling. This causes a noncompaction cardiomyopathy. If physiologically tolerated and does not result in embryonic lethality, the heart is underdeveloped in the post-natal mouse, and there is cardiomyopathic remodeling over time associated with increased TGFβ signaling.